

Zebrafish model for human long QT syndrome

Rima Arnaout^{†‡}, Tania Ferrer[§], Jan Huisken[†], Kenneth Spitzer[§], Didier Y. R. Stainier^{†¶}, Martin Tristani-Firouzi^{§¶}, and Neil C. Chi^{†¶}

[†]Department of Biochemistry and Biophysics, Programs in Developmental Biology, Genetics, and Human Genetics, Cardiovascular Research Institute, University of California, 1550 Fourth Street, San Francisco, CA 94158; [§]Department of Pediatrics and Nora Eccles Harrison Cardiovascular Research and Training Institute, University of Utah, 95 South 2000 East, Salt Lake City, UT 84112; and [¶]Harvard Medical School, 260 Longwood Avenue, Boston, MA 02115

Edited by David E. Clapham, Harvard Medical School, Boston, MA, and approved May 21, 2007 (received for review March 23, 2007)

Long QT syndrome (LQTS) is a disorder of ventricular repolarization that predisposes affected individuals to lethal cardiac arrhythmias. To date, an appropriate animal model of inherited LQTS does not exist. The zebrafish is a powerful vertebrate model used to dissect molecular pathways of cardiovascular development and disease. Because fundamental electrical properties of the zebrafish heart are remarkably similar to those of the human heart, the zebrafish may be an appropriate model for studying human inherited arrhythmias. Here we describe the molecular, cellular, and electrophysiological basis of a zebrafish mutant characterized by ventricular asystole. Genetic mapping and direct sequencing identify the affected gene as *kcnh2*, which encodes the channel responsible for the rapidly activating delayed rectifier K⁺ current (*I_{Kr}*). We show that complete loss of functional *I_{Kr}* in embryonic hearts leads to ventricular cell membrane depolarization, inability to generate action potentials (APs), and disrupted calcium release. A small hyperpolarizing current restores spontaneous APs, implying wild-type function of other ionic currents critical for AP generation. Heterozygous fish manifest overt cellular and electrocardiographic evidence for delayed ventricular repolarization. Our findings provide insight into the pathogenesis of homozygous *kcnh2* mutations and expand the use of zebrafish mutants as a model system to study human arrhythmias.

cardiac | development | *kcnh2* | arrhythmia | electrophysiology

Autosomal dominant *KCNH2* mutations account for ≈45% of mutation-positive long QT syndrome (LQTS) (1, 2). Recessive *KCNH2* mutations are rarely reported, implying that most homozygous mutations are embryonic-lethal (3, 4). The cellular mechanisms underlying embryonic lethality are not known. Although LQTS has been extensively characterized in humans, establishing an animal model would be helpful to identify genes that modify phenotypic expressivity or to screen against compounds that cause acquired forms of LQTS. To date, an appropriate animal model of inherited LQTS does not exist. Transgenic strategies and targeted deletion of genes that regulate rapidly activating delayed rectifier K⁺ current (*I_{Kr}*) and slow delayed rectifier K⁺ current (*I_{Ks}*) in mice fail to produce a significant phenotype (5–7). The mouse heart rate is nearly 10 times faster than that of humans, and thus a distinct cadre of ion channels facilitates ventricular repolarization in mice (5–8).

Although the zebrafish heart is two-chambered, its fundamental electrical properties are remarkably similar to those of humans (9). For example, embryonic and adult heart rates are similar to those of humans (10, 11), and the relationship between QT interval and heart rate parallels that of humans (11). Forward-genetic screens using zebrafish have identified many cardiovascular mutants for analysis (12, 13), thereby revealing critical pathways in cardiovascular development that parallel those of higher vertebrates (14). Large clutch size facilitates positional cloning and other high-throughput experiments using zebrafish embryos and larvae. The role of zebrafish mutants as models of human-inherited arrhythmia has not yet been established.

In this study, we analyze the molecular, cellular, and electrophysiological bases of two recessive mutations that cause ventricular asystole (silent ventricle). The silent ventricle phenotype

is characterized by disrupted intracellular calcium release and can be rescued with an injection of hyperpolarizing current. Like their human counterparts, heterozygous animals exhibit increased sensitivity to QT-prolonging drugs, ventricular action potential (AP) prolongation, and QT interval prolongation on an electrocardiogram.

Results and Discussion

Mutations in *kcnh2* Cause a Silent Ventricle Phenotype and Render *I_{Kr}* Channels Nonfunctional. We identified two alleles (*s213* and *s290*) of a silent ventricle mutant in an ethylnitrosourea forward-genetic screen (15). As early as 33 h postfertilization (hpf), the mutant ventricles do not contract or fill with blood, appearing collapsed. Atrial contraction and morphology appear unaffected. By 48 hpf, both mutant alleles also exhibit pericardial edema and absence of circulation [Fig. 1 *b* and *c* and [supporting information \(SI\) Movies 1 and 2](#)]. After several days, the atrium contracts only weakly, and pericardial edema has increased, ultimately resulting in death by ≈10 days postfertilization, when the larva can no longer survive on oxygen diffusion alone. By contrast, heterozygotes survive to adulthood and are fertile.

We genetically mapped the *s290* mutation to a 1.8-cM region on chromosome 3 and identified a zero-recombinant marker within *kcnh2* (Fig. 1*d*). Sequence analysis of *kcnh2* revealed missense mutations in the *s213* and *s290* mutant alleles, resulting in Ile462Arg and Met521Lys substitutions in the S3 and S5 transmembrane domains, respectively (Fig. 1*e* and *f*). To further test whether *kcnh2* was responsible for the silent ventricle phenotype of the *s213* and *s290* mutants, we knocked down its function by using morpholino antisense oligonucleotides. Injection of 2 ng of an ATG morpholino recapitulated the silent ventricle phenotype in ≈95% of embryos (*n* > 150). Moreover, injecting 100 pg of wild-type *kcnh2* mRNA into *s290* embryos rescued the silent ventricle phenotype in 83% of homozygous mutant embryos (*n* = 47; [SI Fig. 6](#)). Through complementation analysis, we determined that *s213* and *s290* are strong alleles of *bre^{th218}*, which was identified as a mutation in *kcnh2* (16). Together these data indicate that the *s213* and *s290* mutations affect *kcnh2*.

To determine the functional consequences of the disease-causing mutations, we recorded ionic currents from wild-type and mutant Kcnh2 heterologously expressed in *Xenopus* oocytes. Wild-type zebrafish Kcnh2 current displayed biophysical fea-

Author contributions: R.A., T.F., J.H., D.Y.R.S., M.T.-F., and N.C.C. designed research; R.A., T.F., J.H., K.S., M.T.-F., and N.C.C. performed research; R.A., T.F., J.H., D.Y.R.S., M.T.-F., and N.C.C. analyzed data; and R.A., D.Y.R.S., M.T.-F., and N.C.C. wrote the paper.

The authors declare no conflict of interest.

This article is a PNAS Direct Submission.

Abbreviations: hpf, hours postfertilization; LQTS, long QT syndrome; LQT2, LQTS type 2; AP, action potential; *I_{Kr}*, rapidly activating delayed rectifier K⁺ current; *I_{Ks}*, slow delayed rectifiers K⁺ current; SPIM, selective plane illumination microscopy.

[¶]To whom correspondence may be addressed. E-mail: didier.stainier@biochem.ucsf.edu, mfirmouzi@cvrti.utah.edu, or chi@medicine.ucsf.edu.

This article contains supporting information online at www.pnas.org/cgi/content/full/0702724104/DC1.

© 2007 by The National Academy of Sciences of the USA

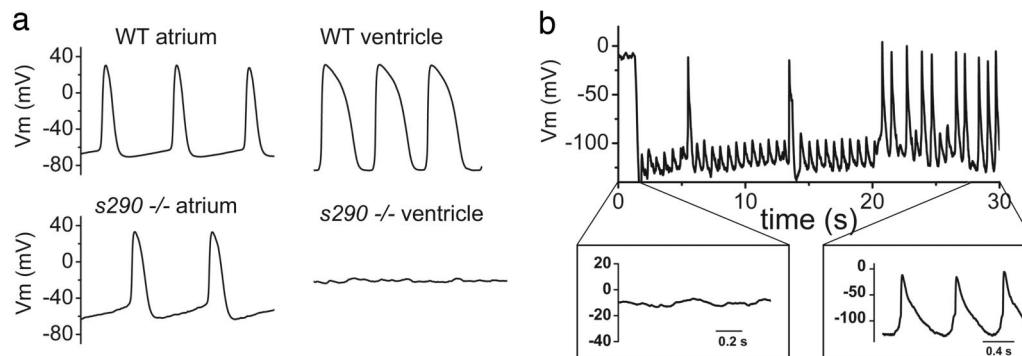


Fig. 3. APs recorded from explanted embryonic zebrafish hearts. (a) (Upper) Representative spontaneous APs recorded from wild-type (WT) atrium (Left) and ventricle (Right) at 48 hpf. (Lower) Spontaneous APs recorded from *kcnh2*^{s290} mutant atrium (Left). Recordings of transmembrane voltage (V_m) from mutant ventricle (Right) revealed marked membrane depolarization and the absence of action potentials. (b) V_m recorded from *kcnh2*^{s290} mutant ventricle. Intracellular injection of hyperpolarizing current (-100 pA) caused membrane hyperpolarization and allowed for the generation of spontaneous APs.

Mutant atria also generated spontaneous APs, although the cycle length, AP duration, and effective refractory period were longer than wild type (SI Table 1). This observation implies that I_{K_r} participates in setting the pacemaker rate and contributes to phase 3 repolarization in the atrium. Recordings from mutant ventricles were markedly abnormal, with a resting V_m of -0.5 ± 3 mV ($n = 10$), compared with -70 mV in wild type (SI Table 1). No spontaneous APs were detected in mutant ventricles, even as the atria were contracting vigorously. This degree of cell membrane depolarization would be expected to inactivate ventricular Ca^{2+} channels responsible for AP upstroke. To determine whether the mutant ventricle was functionally capable of generating APs, we restored the membrane potential with continuous injection of a small negative current (50 – 100 pA). This current caused hyperpolarization of V_m to less than -80 mV, at which point spontaneous APs were consistently elicited (Fig. 3b). The resultant APs were markedly abnormal, with the repolarization phase (see Fig. 3b Inset) provided not by K^+ current, but rather by the injected, hyperpolarizing current. These data suggest that the mutant ventricle is functionally capable of generating APs, but that the complete absence of I_{K_r} causes membrane depolarization, which inactivates L-type Ca^{2+} channels and inhibits AP upstroke.

To further explore the role of I_{K_r} in modulating ventricular APs, we perfused explanted embryonic hearts with high (1 μ M) and low (100 nM) terfenadine concentrations, expecting to cause maximal and submaximal I_{K_r} block, respectively (20). High concentrations of terfenadine (1 μ M) caused progressive depolarization of ventricular V_m (-75 ± 9 to -52 ± 6 mV; $n = 3$) and diminished AP magnitude, and subsequently eliminated electrical activity, similar to the *s213* and *s290* *kcnh2* mutations (SI Fig. 7). Lower concentrations of terfenadine (100 nM) prolonged AP duration by $58 \pm 15\%$ ($n = 4$), resulting in a 2:1 block of external pacing (SI Fig. 7). Thus, a partial I_{K_r} block prolongs AP duration and reduces excitability, whereas a complete I_{K_r} block eliminates excitability in an embryonic zebrafish ventricle. Moreover, these data imply that I_{K_r} is not only critical for repolarization, but is also important for maintaining resting V_m in the embryonic ventricle.

***kcnh2* Homozygous Mutant Ventricle Has Impaired Ca^{2+} Release.** The effect of the null *kcnh2* mutations on cardiac Ca^{2+} cycling was studied in the zebrafish transgenic line *Tg(cmlc2:gCaMP)*^{s878} (N.C.C., R. M. Shaw, B. Jungblut, J.H., R.A., T.F., M.T.-F., L. J. Jan, and D.Y.R.S., unpublished data), which expresses gCaMP, a genetically encoded, voltage-sensitive fluorescent Ca^{2+} sensor (21), using selective plane illumination microscopy (SPIM) (22) to image fluctuating Ca^{2+} in the heart with high

spatial and temporal resolution. To facilitate imaging, contraction was uncoupled from conduction by injection of the silent heart cardiac troponin (*tnt2*) morpholino (23) at the one-cell stage. *In vivo* images were then obtained at 48 hpf. In wild-type *tnt2* morpholino-injected *Tg(cmlc2:gCaMP)*^{s878} hearts, repetitive fluorescent waves representing systolic Ca^{2+} release were visible spreading from the atrium through the atrioventricular junction and into the ventricle (Fig. 4a and SI Movie 3). In *tnt2* morpholino-injected *Tg(cmlc2:gCaMP)*^{s878} *kcnh2*^{s213} and *-kcnh2*^{s290} homozygous mutant embryos, Ca^{2+} waves were visible in the atrium, but no fluorescent changes were detected in the ventricle (Fig. 4b and SI Movie 4). These data indicate that Ca^{2+} release and/or reuptake is impaired in *kcnh2* mutant ventricular myocytes as a consequence of absent I_{K_r} .

***kcnh2* Heterozygous Animals Display Abnormal Ventricular Repolarization.** Heterozygous *kcnh2*^{s213} and *kcnh2*^{s290} embryos appear phenotypically similar to their wild-type siblings. However, when coexpressed with wild-type *kcnh2* at equimolar mRNA concentrations, Ile462Arg and Met521Lys *kcnh2* caused reduced current consistent with dominant-negative suppression of wild-type K_{cnh2} channel function (data not shown), suggesting that I_{K_r} function may be reduced in the heterozygous state. To determine whether heterozygous fish, like their human LQT2 counterparts, are especially sensitive to I_{K_r} -blocking drugs, we bathed 48 hpf embryos with terfenadine (24). At increasing concentrations, terfenadine causes bradycardia, a 2:1 atrioventricular block, and ultimately ventricular asystole in embryonic zebrafish hearts (11, 16, 25). For these experiments, high concentrations of terfenadine were required to observe an effect given that the compound must diffuse through the embryo. We chose a terfenadine concentration (32 μ M) that was below the threshold (85 μ M, 2-h incubation) for development of a 2:1 block in wild-type embryonic hearts. Wild-type-looking embryos from increased *kcnh2*^{s213} and *kcnh2*^{s290} heterozygous fish were incubated in 32 μ M terfenadine, scored for the development of a 2:1 block, and genotyped. For each allele, 100% ($n = 12$) of the heterozygotes developed a 2:1 heart block, as opposed to none of the homozygous wild-type embryos ($n = 9$). In this setting, heart block presumably occurs as a consequence of refractory ventricular myocardium, rather than a block at the level of the atrioventricular node/groove. Likewise, children with severe LQTS often present in the newborn period with a functional 2:1 atrioventricular heart block because of markedly delayed ventricular repolarization (3).

Our data suggest that *kcnh2*^{s213} and *kcnh2*^{s290} heterozygous embryos have reduced repolarization reserve. To determine whether heterozygotes are distinguishable from wild type at the

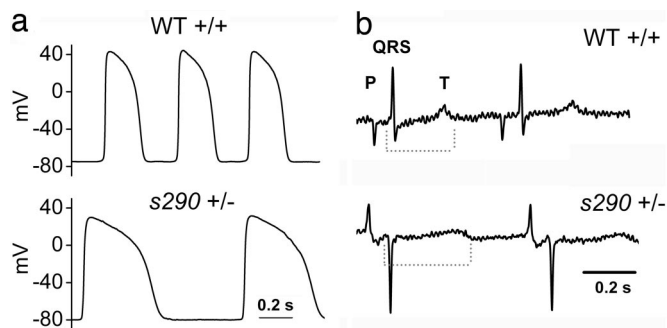


Fig. 5. Heterozygous *kcnh2* zebrafish manifest delayed ventricular repolarization. (a) APs recorded from 48 hpf heterozygous ventricle show increased AP duration compared with wild-type (see Results). (b) Representative electrocardiograms recorded from anesthetized, paralyzed wild-type and heterozygous adult zebrafish. Dashed line indicates duration of QT interval. QT corrected for heart rate (see Materials and Methods) was 396 and 467 msec for the exemplar wild-type and heterozygote, respectively.

is nearly equal, the frequency of homozygous mutations is disparate. The incidence of homozygous mutations in *KCNQ1* (also known as Jervell–Lange–Nielsen syndrome) is $\approx 1:500,000$, with affected individuals manifesting severe QT prolongation and sensorineural deafness (26). By contrast, viable humans with homozygous *KCNH2* mutations are only rarely described in the literature, most likely as a consequence of embryonic lethality. Lethality in zebrafish *kcnh2* mutants occurs as the result of chronic membrane depolarization, with the resultant inability to generate APs and appropriately cycle intracellular Ca^{2+} . The precise cellular mechanisms underlying embryonic lethality in human homozygous LQT2 remain to be determined.

Heterozygous mutations in zebrafish *kcnh2* recapitulate the human LQTS phenotype as manifested by AP prolongation and prolonged QT interval, and thereby define the first animal genetic model of human LQT2. A major unanswered question within the LQTS field is why one affected individual manifests marked QT prolongation, whereas their sibling harboring the identical mutation appears phenotypically unaffected. As a model of LQT2, the zebrafish mutants described here offer the opportunity to analyze a large number of offspring with an identical *kcnh2* mutation and to ultimately identify comodifying genes that influence phenotypic expressivity in humans.

Materials and Methods

Zebrafish Strains and Lines. Zebrafish were raised under standard laboratory conditions at 28°C. We used the following lines: *kcnh2*^{s213} (15), *kcnh2*^{s290} (15), *mnt2*^{b109} (23), *Tg(cmlc2:gCaMP)*^{s878} (N.C.C., R. M. Shaw, B. Jungblut, J.H., R.A., T.F., M.T.-F., L. J. Jan, and D.Y.R.S., unpublished data), and *Tg(cmlc2:eGFP)* (27).

Pharmacological Treatment. A 30-mM stock of terfenadine (Sigma–Aldrich, St. Louis, MO) in DMSO was diluted in embryo water. Embryos at 48 hpf were dechorionated, if not already hatched, and incubated in 1 to 85 μM terfenadine in embryo water. Control embryos were incubated in 1% DMSO in embryo water.

Mapping. We mapped the mutation to linkage group 3 by using a set of simple sequence-length polymorphism markers. For fine mapping, 840 mutant embryos were tested with simple sequence-length polymorphism markers in the critical region (Fig. 1d). *kcnh2* complementary DNA was isolated, sequenced, and analyzed from wild-type and the two mutant alleles. To genotype mutant embryos, we used a BsmA1 restriction site for restriction fragment length polymorphism analysis of *kcnh2*^{s213} and an Sml1

restriction site for restriction fragment length polymorphism analysis of *kcnh2*^{s290}.

Video Recording/Microscopy. Brightfield pictures and videos were taken by using a Stemi SV11 dissecting microscope (Carl Zeiss, Thornwood, NY). Videos were captured by using a standard CCD camera at 20 frames per sec.

SPIM. Videos of the cardiac conduction wave were recorded with SPIM (22). The attenuated 488-nm laser line from a DPSS laser (Sapphire 30 mW; Coherent, Santa Clara, CA) was focused to a 6- μm -thick light sheet. The sample was oriented such that a thin slice of atrium, AV canal, and ventricle was illuminated. The fluorescence was collected with a (20 \times /0.5) objective lens (Leica, Wetzlar, Germany) and an emission filter (HQ 525/50m; Chroma Technology Corp., Rockingham, VT) and imaged on an EM-CCD camera (DV885, 8- μm pixel size, binning 2; Andor, Belfast, Northern Ireland). Only a small area of the chip was read out, yielding a frame rate of ≈ 90 frames per sec. The microscope and camera were controlled with a Labview (National Instruments, Austin, TX) program, and images were saved in a binary format. After acquisition, the video sequences were analyzed with Matlab (The Mathworks, Natick, MA). In each sequence, several areas 15 \times 15 pixels wide (i.e., 12 \times 12 μm) were selected, and the intensity in these areas was plotted over time. All plots were semilogarithmic and identically scaled.

Morpholino Injections (*tnnt2* and *kcnh2*). We used a morpholino oligonucleotide targeted against the translational start site of *kcnh2* (National Center for Biotechnology Information sequence no. NM_212837) with the following sequence: 5′-CGCGTGGACA-GATTCAAGAGCCCTC-3′. The *silent heart* (*sih/tnnt2*) ATG morpholino was used as previously described (23).

AP Recordings from Embryonic Heart. Forty-eight hpf embryos were dechorionated and anesthetized with 0.02% tricaine for 1 to 2 min. The heart was dissected from the thorax *en bloc* by using fine forceps and transferred to the recording chamber. Only spontaneously beating whole hearts were studied. All experiments were performed at 22–24°C. The recording chamber was perfused with solution containing 140 mM NaCl, 4 mM KCl, 1.8 mM CaCl_2 , 1 mM MgCl_2 , 10 mM glucose, and 10 mM Hepes (pH 7.4). Suction pipettes were made from borosilicate capillary tubes (8,250 glass; A-M Systems, Sequim, WA) and fire-polished to obtain resistances of 6–9 M Ω when filled with 120 mM KCl, 5 mM EGTA, 5 mM K_2ATP , 10 mM Hepes, and 5 mM MgCl_2 (pH 7.2). Transmembrane potential (V_m) was measured by using an Axoclamp 2A amplifier (Molecular Devices, Sunnyvale, CA) in the bridge mode. V_m was measured with the disrupted patch technique. The pipette was positioned adjacent to the heart and a seal was formed by application of minimal suction. Using this technique, stable spontaneous APs were recordable for up to 2 h. Ventricular APs were generated by spontaneous electrical activity emanating from the atrium. V_m was filtered at 10 kHz and digitized at a sampling frequency of 20 kHz with a 12-bit analog-to-digital converter (Digidata 1322A Interface; Molecular Devices). AP duration from a series of five or more APs was calculated as the time interval between the peak maximum upstroke velocity (phase 0) and the time at 90% of repolarization (APD_{90}). To determine the effective refractory period, the heart was paced by injecting pulses of depolarizing current (1.5 \times threshold, 3 msec duration) at a cycle length of 350 msec for the atrium and 400 msec for the ventricle. Ten consecutive stimuli were followed by a single premature stimulus at progressively shorter coupling intervals.

Measurement of Electrocardiograms. Electrocardiograms were performed on adult zebrafish by using a protocol modified from

